

Polyion Complex Micelles Formed From Glucose Oxidase and Comb-Type Polyelectrolyte With Poly(ethylene glycol) Grafts

AKIFUMI KAWAMURA,¹ CHIE KOJIMA,¹ MICHIIRO IJIMA,² ATSUSHI HARADA,¹ KENJI KONO¹

¹Department of Applied Chemistry, Graduate School of Engineering, Osaka Prefecture University, 1-1 Gakuen-cho, Naka-ku, Sakai, Osaka 599-8531, Japan

²Department of Materials Chemistry and Bioengineering, Oyama National College of Technology, 771 Nakakuki, Oyama, Tochigi 323-0806, Japan

Received 4 December 2007; accepted 7 March 2008

DOI: 10.1002/pola.22739

Published online in Wiley InterScience (www.interscience.wiley.com).

ABSTRACT: The comb-type polyelectrolyte, poly(ethylene glycol)-*graft*-poly(allyl amine) (PEG-*g*-PAA), was synthesized to prepare polyion complex (PIC) micelles with *Aspergillus Niger* Glucose oxidase (GOD). Even after mixing GOD and PEG-*g*-PAAs with various PEG contents, the resulting mixtures remained transparent but the mixture of GOD and PAA homopolymer immediately precipitated. In the mixtures prepared with a stoichiometric mixing ratio, the formation of PIC micelles with a core-shell structure was suggested from dynamic and static light scattering measurements. Glucose, the substrate for GOD, could easily diffuse into the PIC micelles, and the GOD molecules were active even in the core of the PIC micelles. GOD didn't lose its enzymatic activity through entrapment into the PIC micelles. © 2008 Wiley Periodicals, Inc. *J Polym Sci Part A: Polym Chem* 46: 3842–3852, 2008

Keywords: biomaterials; complex micelles; enzymes; graft copolymers; polyion

INTRODUCTION

Polyion complex (PIC) formation is an interesting mechanism for self-organizing supramolecular structures, and has gained high practical relevance for coatings, membranes with special separation properties, or for microencapsulation.¹ The mixture of oppositely charged polyelectrolyte solutions leads to spontaneous aggregation. Size and colloid stability depend on the molar mixing ratio of the charged units, ionic strength, and pH in particular, when PICs are prepared at a 1:1 charge stoichiometry. Some

attempts have been made to control the colloid stability of PICs at the nanoscopic or mesoscopic size level. The use of block ionomers composed of a polyelectrolyte block and a nonionic block for polyion complexation effectively improves colloid stability.² Mixing a pair of oppositely charged block ionomers forms core-shell type PIC micelles, in which the PIC core is surrounded by nonionic blocks.³ PIC micelles are formed not only from a pair of oppositely charged block ionomers but also from the mixture of block ionomers with oppositely charged compounds, for example, synthetic polymers, surfactants, and natural bioactive molecules including DNA and enzymes.^{2,4} PIC micelles entrapping bioactive molecules have received considerable attention from fields such as the nanometric-scaled containers (nano-containers).⁵

Correspondence to: A. Harada (E-mail: harada@chem.osakafu-u.ac.jp)

Journal of Polymer Science: Part A: Polymer Chemistry, Vol. 46, 3842–3852 (2008)
© 2008 Wiley Periodicals, Inc.

PIC micelles might form by mixing a graft copolymer having a polyelectrolyte main chain, a comb-type polyelectrolyte, and oppositely charged compounds. There are a few reports on water-soluble complexes obtained from comb-type polyelectrolytes and enzyme molecules,⁶ although the studies on the complexation of DNA with a comb-type polyelectrolyte have been extensively carried out for applications in gene therapy and surface modification.⁷ In addition, the functionality of enzymes through complexation with comb-type polyelectrolytes has never been reported. Also, comb-type polyelectrolyte has advantage in the entrapment of enzyme molecules in the micelles. In the case of using block copolymer, the core radius of the formed micelles was determined by the length of charged block.⁸ Also, the balance between core-forming charged block and shell-forming nonionic block was important for the formation of PIC micelles. That is, to incorporate large enzyme into PIC micelles, nonionic block as well as charged block also have to be prolonged. The synthesis of such block copolymer having longer blocks is difficult compared with the synthesis of comb-type polyelectrolyte. Comb-type polyelectrolyte could control both of the main chain length and grafting degree, and could adjust to enzymes with the various sizes.

In this study, the comb-type polyelectrolyte, poly(ethylene glycol)-*graft*-poly(allyl amine) (PEG-*g*-PAA), composed of poly(allyl amine) as the cationic main chain and poly(ethylene glycol) as the graft chain was synthesized. Then, PIC micelles formed from PEG-*g*-PAA and *Aspergillus Niger* glucose oxidase (GOD), which is the anionic enzyme and is used as sensing part in biosensor, and were evaluated by using light scattering techniques. Furthermore, it was confirmed that GOD maintained its enzymatic activity even in the core of the micelles.

EXPERIMENTAL

Materials

α -acetal- ω -hydroxyl-poly(ethylene glycol) ($M_n = 9000$) was synthesized as previously described.⁹ 4-nitrophenyl chloroformate was purchased from Aldrich (Milwaukee, WI), and used without further purification. Triethylamine and D-(+)-glucose were purchased from Kishida Chemical (Osaka, Japan), and used for further purification. Poly(allyl amine) hydrochloride ($M_n :$

15,000) was purchased from Nitto Boseki Co., Ltd. (Tokyo, Japan), and used after deprotonation. GOD was purchased from MP Biomedicals, Inc, and used without further purification. Horse radish peroxidase and *o*-dianisidine dihydrochloride were purchased from Wako Pure Chemical Industries (Osaka, Japan); and used without further purification.

Synthesis of α -Acetal- ω -Nitrophenyl Carbonate-Poly(ethylene glycol)

α -acetal- ω -hydroxyl-poly(ethylene glycol) [8 g (0.89 mmol)] and triethylamine [354 mg (3.50 mmol)] were dissolved in 15 mL distilled THF. 4-nitrophenylchloroformate [484 mg (2.40 mmol)] in 4 mL distilled THF was added dropwise to the PEG solution. After 7 days, THF was removed under vacuum, and chloroform was added to the residue. Distilled water was added to the solution, and the chloroform phase was collected after stirring, followed by pouring into diethyl ether to precipitate the polymer. The obtained polymer was dried *in vacuo*, and freeze-dried using benzene. The successful introduction of the NPC group onto the end of poly(ethylene glycol) (PEG) was confirmed by ¹H NMR. The yield of the obtained polymer α -acetal- ω -nitrophenylcarbonate-poly(ethylene glycol) (PEG-NPC) after purification was 78%.

Graft Copolymerization of α -Acetal- ω -Nitrophenyl Carbonate-Poly(ethylene glycol) With Poly(allyl amine)

Poly(allyl amine) and PEG-NPC were separately dissolved in methanol containing 25 mM LiCl. The PEG-NPC solution was added dropwise to the PAA solution. The reaction mixture was stirred for 3 days, and then methanol was removed under vacuum. The obtained compound was dissolved in aqueous HCl (pH 4.5), and dialyzed against distilled water using Seamless Cellulose Tubing (molecular weight cut off = 12,000–14,000). Finally, unreacted PEG-NPC was removed by ion-exchange chromatography (SP Sepharose, Amersham Bioscience). To confirm the introduction of PEG graft chains into PAA and the removal of unreacted PEG, gel permeation chromatography (GPC) measurements were carried out in 0.5M CH₃COOH/CH₃COONa buffer with 0.1M NaCl (pH 5.0) using a column combination of TSK gel G6000PW and TSK gel G4000PW (Tosoh Co.,

Tokyo, Japan) at 40 °C. The flow rate was 0.5 mL/min, and the elution signal was detected by assessing the refractive index.

Preparation of GOD-Incorporated PIC Micelles

Appropriate amounts of GOD and PEG-*g*-PAA were separately dissolved in Tris-HCl buffer solution (Tris, 50 mM, pH 7.4). After filtration through a 0.1- μ m filter to remove dust, these solutions were mixed in various mixing ratios at 25 °C to form complexes. The number of primary amino groups in PEG-*g*-PAA against the total number of aspartic acid and glutamic acid residues in GOD (Mixing ratio (MR) = [amine in PEG-*g*-PAA]/[Asp and Glu in GOD]) was used as a major parameter in these experiments. The mixtures were stored at 25 °C for longer storage (more than 12 h after mixing).

Dynamic Light Scattering Measurement

Dynamic light scattering (DLS) measurements were carried out using a DLS-6000AS (Otsuka Electronics Co., Ltd., Osaka, Japan). Vertically polarized light at 488 nm from the Ar ion laser was used as the incident beam. All measurements were performed at 25 \pm 0.2 °C. In the DLS measurements, the general formula for the photoelectron count time correlation function had the form:

$$g^{(2)}(\tau) = 1 + \beta |g^{(1)}(\tau)|^2 = 1 + \beta \exp(-2\Gamma\tau) \quad (1)$$

where $g^{(2)}(\tau)$ is the normalized second order correlation function, β is a parameter of the optical system (constant), $g^{(1)}(\tau)$ is the normalized first order correlation function, τ is the delay time, and Γ is the average characteristic line width. $g^{(1)}(\tau)$ can be expressed by the following equation:

$$g^{(1)}(\tau) = \int G(\Gamma) \exp(-\Gamma\tau) d\Gamma \quad (2)$$

where $G(\Gamma)$ is the distribution function of Γ . The autocorrelation functions were analyzed using the method of cumulants in which

$$g^{(1)}(\tau) = \exp[-\Gamma\tau + (\mu_2/2)\tau^2 - (\mu_3/3!)\tau^3 + \dots] \quad (3)$$

yielding an average line width Γ , and a variance (polydispersity index) μ_2/Γ^2 . In the cumulant

approach, the z-averaged diffusion coefficient, D , was obtained from the average line width, Γ , based on the following equation:

$$\Gamma = Dq^2 \quad (4)$$

$$q = 4\pi n \sin(\theta/2)\lambda \quad (5)$$

where q is the magnitude of the scattering vector, and θ is the detection angle. The corresponding hydrodynamic radius, R_h , can then be calculated using the Stokes-Einstein equation:

$$R_h = k_B T / (6\pi\eta D) \quad (6)$$

where k_B is the Boltzmann constant, T is the absolute temperature, and η is the solvent viscosity.

Static Light Scattering Measurement

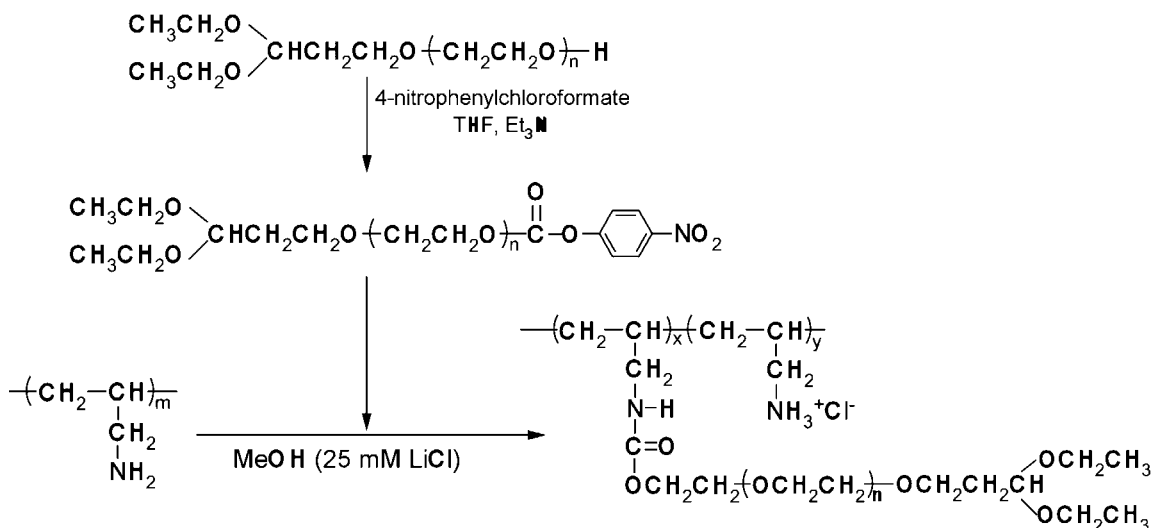
Static light scattering (SLS) measurements were carried out using a DLS-7000K (Otsuka Electronics Co., Ltd., Osaka, Japan). The light scattered by a dilute polymer solution may be expressed by the following equation:

$$KC/\Delta R(\theta) = (1/M_{w,app})(1 + q^2 R_g^2/3) + 2A_2 C$$

Here C is the concentration of polymer, $\Delta R(\theta)$ is the difference between the Rayleigh ratio of the solution and that of the solvent, $M_{w,app}$ is the apparent weight average molecular weight, R_g is the mean-square radius of gyration, A_2 is the second virial coefficient, and K ($4\pi^2 n^2 (dn/dc)^2 / (N_A \lambda^4)$) (N_A is Avogadro's number). The known Rayleigh ratio of benzene was used as a calibration standard. The increments of refractive index, dn/dc , of the solutions were measured using a DRM-1020 double-beam differential refractometer (Otsuka Electronics Co., Ltd., Osaka, Japan).

Evaluation of GOD Activity

The enzymatic activity of GOD was evaluated using the peroxidase/*o*-dianisidine method using Wallac 1420 ARVOSx (Perkin-Elmer, Inc., MA).¹⁰ The reaction rate of GOD was determined by monitoring the change in absorbance at 450 nm after mixing the solutions containing GOD, glucose, peroxidase, and *o*-dianisidine.



Scheme 1. Synthetic route of poly(ethylene glycol)-*graft*-poly(allyl amine).

RESULTS AND DISCUSSION

The synthetic route of the graft copolymer, PEG-*g*-PAA is illustrated in Scheme 1. First, the heterobifunctional poly(ethylene glycol), α -acetal- ω -hydroxyl-poly(ethylene glycol) (PEG-OH), was synthesized according to a previous report; and then, the hydroxyl group was converted into a nitrophenyl carbonate group by reacting with 4-nitrophenyl chloroformate. The obtained PEG-NPC was introduced to PAA as graft chains through the urethane bond formation reaction between the NPC group of PEG-NPC and the primary amino group of PAA. The synthesis of graft copolymers was confirmed from the GPC and ^1H NMR analyses. Unimodal elution profiles were observed in the GPC analysis for all samples as shown in Figure 1. There was no original peak for PEG-OH in the graft copolymers, and the unreacted PEG, which eluted at 20.2 mL, was completely removed through the purification process using an ion exchange column. In addition, the retention volume of the graft copolymers decreased with an increasing PEG content of the graft copolymers, demonstrating increments in molecular weight. The molecular weight distribution (M_w/M_n) of the obtained polymers was determined from the calibration curve using PEG standards, and is summarized in Table 1. All of the obtained graft copolymers had a moderate molecular weight distribution. To confirm the grafting of PEG to PAA, and the composition of the graft copolymers; ^1H NMR measurements were carried out.

Figure 2 shows the ^1H NMR spectra of PEG-*g*-PAA, PAA, and PEG-NPC. From the signals of the benzene protons at 7.4, 8.3 ppm and methylene protons next to the carbonate group at 4.4 ppm, the successful introduction of the *p*-nitrophenyl carbonate group to the PEG-OH was confirmed. By reacting PEG-NPC with PAA, the signal of the *p*-nitrophenyl carbonate group disappeared. The peak of the methylene proton next to the urethane bond newly appeared at 4.2 ppm, demonstrating the formation of a urethane bond through the grafting reaction. The grafting ratio of PEG was determined from the peak area ratio of the methylene proton next to the urethane bond (4.2 ppm) and the methylene proton next to the amino groups of the PAA unit (2.6 ppm). The determined PEG contents of each graft copolymer are summarized in Table 1. The obtained PEG-*g*-PAAs were used in the experiments of complexation with glucose oxidase except for PEG₁-*g*-PAA. Because PEG₁-*g*-PAA includes PAA homopolymer, and considering the various PEG contents, there is the possibility that it will exhibit a complicated complexation behavior. Also, the number of charged residues per a polymer for the obtained polymers were calculated to be 152 for PEG₅-*g*-PAA, 146 for PEG₈-*g*-PAA, 141 for PEG₁₂-*g*-PAA, and 133 for PEG₁₇-*g*-PAA, respectively.

The complexation of PEG-*g*-PAA with different enzymes was evaluated using GOD from *Aspergillus Niger*, which is a rigid dimeric glycoprotein (molecular weight, 186,000 Da) containing one tightly bound FAD molecule.¹⁰ DLS

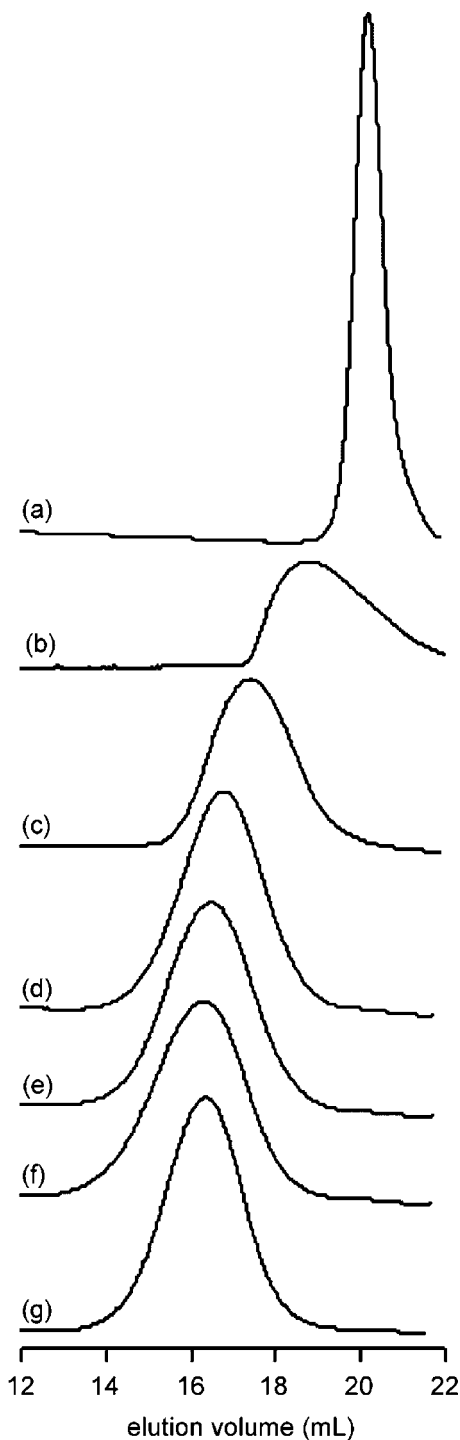


Figure 1. GPC charts of acetal-PEG-OH ($M_n = 9000$) (a), PAA homopolymer (b), PEG₁-*g*-PAA (c), PEG₅-*g*-PAA (d), PEG₈-*g*-PAA (e), PEG₁₂-*g*-PAA (f), and PEG₁₇-*g*-PAA (g).

measurements were performed for solutions of GOD/PEG-*g*-PAA complexes prepared using various MRs in the range of 0.1–3.0, and in which MR related to the ratio of the number of the

amino groups in PEG-*g*-PAA against the total number of aspartic acid and glutamic acid residues in GOD ($MR = [\text{amino group in PEG-}g\text{-PAA}]/[\text{Asp and Glu in GOD}]$). When mixing GOD with PAA homopolymer at a ratio of $0.4 \leq MR \leq 3.0$, the mixtures formed larger aggregates (precipitates). On the other hand, the mixed solutions of GOD and PEG-*g*-PAA showed no precipitation, and remained transparent solutions even after overnight storage. DLS measurements were carried out for these transparent solutions of PEG-*g*-PAA/GOD complexes. Figure 3 shows the change in scattering intensity with the change in the MR. In spite of the composition of PEG-*g*-PAA, the scattering intensities increased with an increase in MR values, and the maximum of scattering intensity was observed at $0.5 \leq MR \leq 0.75$. There were several reports on stoichiometry of the complexation evaluated from the change in light scattering intensity.^{8,11} According to their reports, the profile of changing scattering intensity as shown in Figure 3 indicates that the stoichiometric mixing ratio of the complexation between GOD and PEG-*g*-PAA was $0.5 \leq MR \leq 0.75$, since the scattering intensity is sensitive against the change in molecular mass of solute. The information on the stoichiometry was obtained from not only scattering intensity from but also cumulant diameter and polydispersity index. Figure 4 shows the changes in the cumulant diameter and polydispersity index (μ_2/Γ^2) according to the MR. When mixing GOD with any PEG-*g*-PAA, the maximum change in the cumulant diameter occurred at $MR = 0.5$, and a slight increase and decrease in diameter were observed in the range of $0.1 \leq MR < 0.5$ and $0.5 < MR \leq 3.0$, respectively. Considering experimental errors, the cumulant diameter did not significantly change, in particular in the range $0.5 < MR \leq 3.0$. In addition, the polydispersity index decreased from 0.25 to 0.1 with an increment in MR from 0.1 to 0.5, and then remained constant in the region of $0.5 \leq MR \leq 3.0$. Similar changes of the polydispersity index according to the MR were observed for the PIC micelles from egg white lysozyme and poly(ethylene glycol)-*b*-poly(α,β -aspartic acid) [PEG-P(Asp)].^{4f} In the case of lysozyme/PEG-P(Asp) complexes, increasing the ratio of PEG-P(Asp) to stoichiometric MR resulted in a decrease of the polydispersity index. In this MR range, lysozyme/PEG-P(Asp) complexes showed cooperative micellization, that is, the stoichiometric micelles and free

Table 1. Synthesis of Poly(ethylene glycol)-*g*-poly(allyl amine) (PEG-*g*-PAA)

Code	PEG Content in Feed		PEG Content ^c		M_n^d	M_w/M_n^e
	mol % ^a	Chains ^b	mol % ^a	Chains ^b		
PEG ₁₇ - <i>g</i> -PAA	20	32	17	27	258,000	1.79
PEG ₁₂ - <i>g</i> -PAA	15	24	12	19	187,000	1.82
PEG ₈ - <i>g</i> -PAA	10	16	8	13	137,000	1.80
PEG ₅ - <i>g</i> -PAA	7	11	5	8	89,000	1.92
PEG ₁ - <i>g</i> -PAA	2	3	1	1	31,000	1.84

^a mol % to the allylamine unit.

^b Number of chains per PAA chain.

^c Determined from ¹H NMR.

^d Calculated from the PEG content of the obtained graft copolymers using the M_n of PEG (9,000 g/mol) and PAA (15,000 g/mol).

^e Determined from the calibration curve using PEG standards.

lysozymes coexisted, and the ratio of micelles increased with an increasing PEG-P(Asp) ratio. Because of the considerably high molecular mass of the micelles compared with that of the lysozymes, the cumulant diameter and polydispersity index mainly reflected the size of the micelles and the ratio of the micelles, respectively. GOD/PEG-*g*-PAA complexes presented similar changes to those shown in Figure 4, and these changes might indicate that the stoichiometric MR was 0.5. However, the cumulant diameter of GOD/PEG-*g*-PAA complexes increased with an increasing MR, although lysozyme/PEG-P(Asp) complexes retained a constant diameter. This difference might be explained by the differences in molecular weights of the enzyme and the polymer between GOD/PEG-*g*-PAA complexes and lysozyme/PEG-P(Asp) complexes. The molecular weight of the lysozyme and PEG-P(Asp) were 14,300 and 15,000, respectively. In contrast, the molecular weights of GOD and PEG-*g*-PAA were 186,000 as described above and more than 89,000, respectively, as summarized in Table 1; and GOD and PEG-*g*-PAA had significantly higher molecular weights than the lysozyme and PEG-P(Asp). The scattering intensity from un-complexed GOD was not negligible, and the cumulant diameter might exhibit a slightly smaller value than that of the complexes at stoichiometric MR. When the complexes were prepared with an excess of polymers over the stoichiometric MR, both the lysozyme/PEG-P(Asp) complexes and GOD/PEG-*g*-PAA complexes retained almost constant polydispersity indices. Within that MR region, complex formation might be noncooperative for both the lysozyme/PEG-P(Asp) complexes and GOD/PEG-*g*-PAA complexes. The following experiments were

carried out with the GOD/PEG-*g*-PAA complexes prepared at a stoichiometric MR 0.5.

Figure 5(a) shows the relationship between the average characteristic line width (Γ) and the square of the scattering vector (q^2). For the spherical particles, the Γq^2 ($= D$) values should be independent of the scattering vector because of the undetectable rotational motion. The correlation coefficients for all the mixtures were greater than 0.998, demonstrating a very nice linearity. This linear relationship between Γ and q^2 was consistent with the formation of spherical micelles. Figure 5(b) shows the dependence of the diffusion coefficient (D) on concentration. It was obvious that the D values were independent of the concentration. An increase in concentration induced no formation of secondary aggregates, that is, the cluster of micelles. This indicated that the steric repulsions of the PEG graft chains effectively prevented the aggregation of the complexes. These DLS results (Fig. 5) suggested the formation of core-shell type PIC micelles, in which the PIC core was composed of a PAA main chain and GOD was surrounded by PEG graft chains. In addition, the D value at the infinite dilution (D_0) was determined from Figure 5(b), and the hydrodynamic radius (R_h) was calculated using the Stokes-Einstein equation (eq 6). The obtained D_0 and R_h values are summarized in Table 2. There were no significant differences in R_h values for the micelles prepared from PEG-*g*-PAA with various PEG contents. This might be due to no differences in the lengths of the PAA main chain and the PEG graft chain, since PEG-*g*-PAA was synthesized from the same PAA and PEG.

The apparent molecular mass ($M_{w,app}$) and radius of gyration (R_g) of the GOD/PEG-*g*-PAA

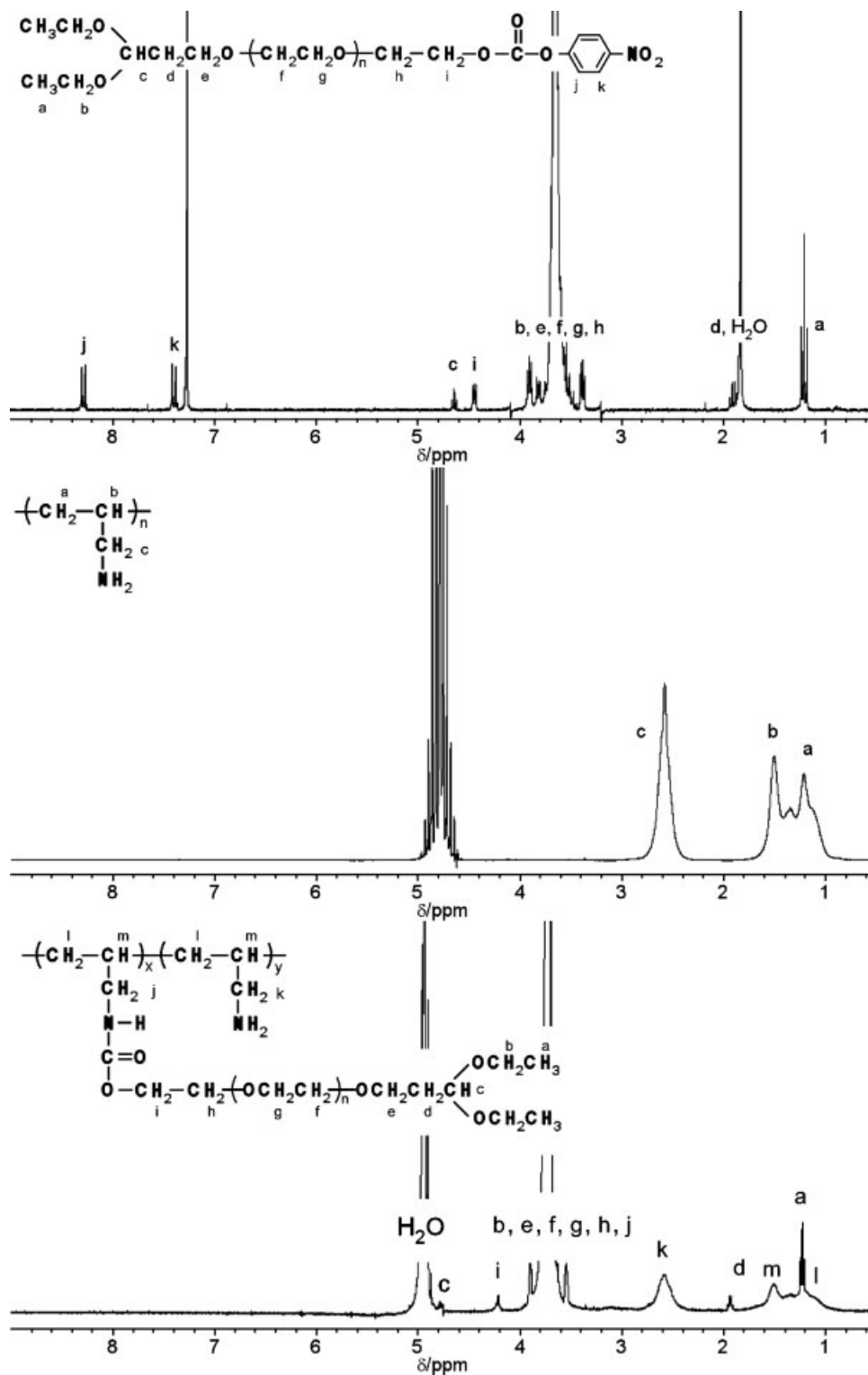


Figure 2. ¹H NMR spectra of PEG-NPC in CDCl₃, PAA in D₂O, and PEG-g-PAA in D₂O.

complexes were determined from Zimm plots of SLS measurements. The obtained $M_{w,app}$, R_g and A_2 were summarized in Table 3. From these

values, the association number of GOD and PEG-g-PAA and the ratio of the R_g to the R_h value (R_g/R_h) were calculated and also summar-

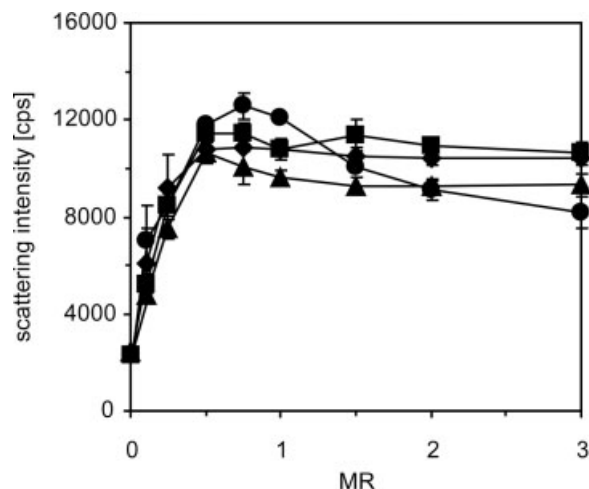


Figure 3. Change in scattering intensity with mixing ratio MR for GOD/PEG-*g*-PAA complexes. Detection angle, 90°; temperature, 25.0 ± 0.2 °C; GOD concentration, 1.0 mg/mL. Symbols, ●, PEG₅-*g*-PAA; ▲, PEG₈-*g*-PAA; ■, PEG₁₂-*g*-PAA; ◆, PEG₁₇-*g*-PAA).

ized in Table 3, in which the association numbers were calculated from the $M_{w,app}$ by using the molecular weight of PEG-*g*-PAA summarized in Table 1 and GOD (186,000 g/mol) based on the assumption that the micelles were formed at the loading ratio (MR = 0.5). The $M_{w,app}$ of the GOD/PEG-*g*-PAA complexes increased with an increase in PEG content of PEG-*g*-PAA. The association number of GOD also decreased with an increase in PEG content of PEG-*g*-PAA. In the formation of PIC micelles, polyelectrolyte complexation is attractive force and induces the increase in the association number.^{4a} However, increasing the association number, the steric repulsion among PEG graft chains also increases, which is thermodynamical disadvantage. The association number is determined by thermodynamical balance between attractive force and conformational disadvantage. Consequently, in the case of the GOD/PEG-*g*-PAA complexes, the increase in PEG content of PEG-*g*-PAA might induce the decrease in the association number. Indeed, the number of PEG graft chain per a complex was no significant dependence to PEG content of graft copolymer compared with the difference in the association number summarized in Table 3, and calculated to be 50–75 chains per a complex. In contrary, the weight fraction of PEG in the complex increased with an increase in PEG content of graft copolymer. This effect was observed for the A_2 values, which mainly reflect the excluded vol-

ume effect. The PAA main chain and GOD form the core region of the complex, which might have a small influence on an excluded volume. The PEG graft chain has a major contribution to the excluded volume of the complex. The GOD/PEG-*g*-PAA complex prepared from PEG-*g*-PAA with higher PEG content had larger A_2 values as summarized in Table 3. Also, it is known that the R_g/R_h value for a hard sphere is 0.775.¹²

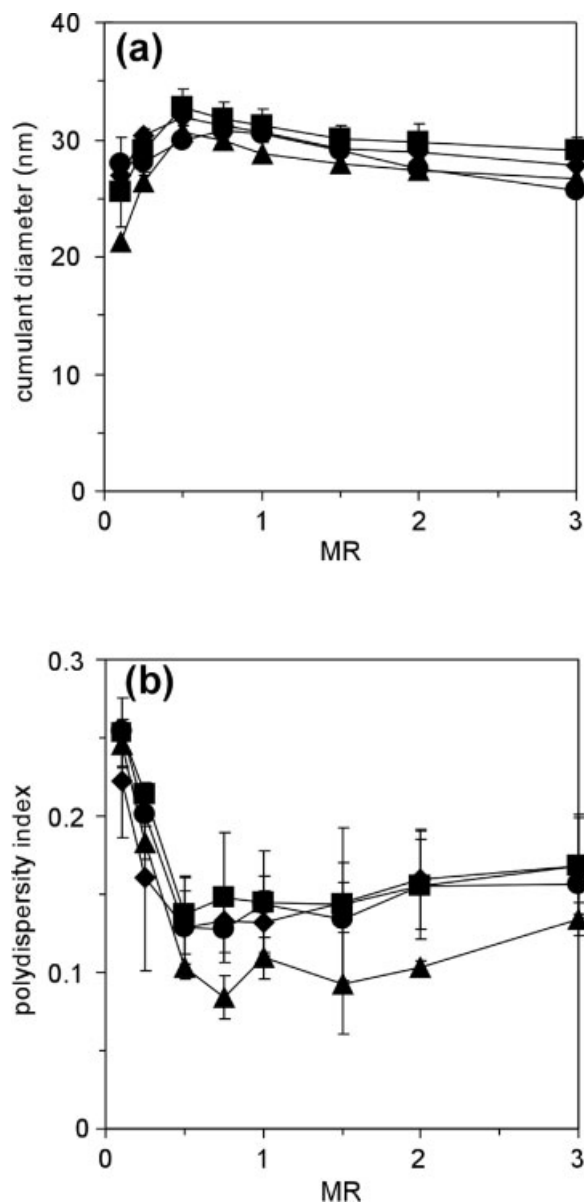


Figure 4. Changes in the cumulant diameter (a) and the polydispersity index (b) according to mixing ratio MR for GOD/PEG-*g*-PAA complexes. Detection angle, 90°; temperature, 25.0 ± 0.2 °C; GOD concentration, 1.0 mg/mL. Symbols, ●, PEG₅-*g*-PAA; ▲, PEG₈-*g*-PAA; ■, PEG₁₂-*g*-PAA; ◆, PEG₁₇-*g*-PAA).

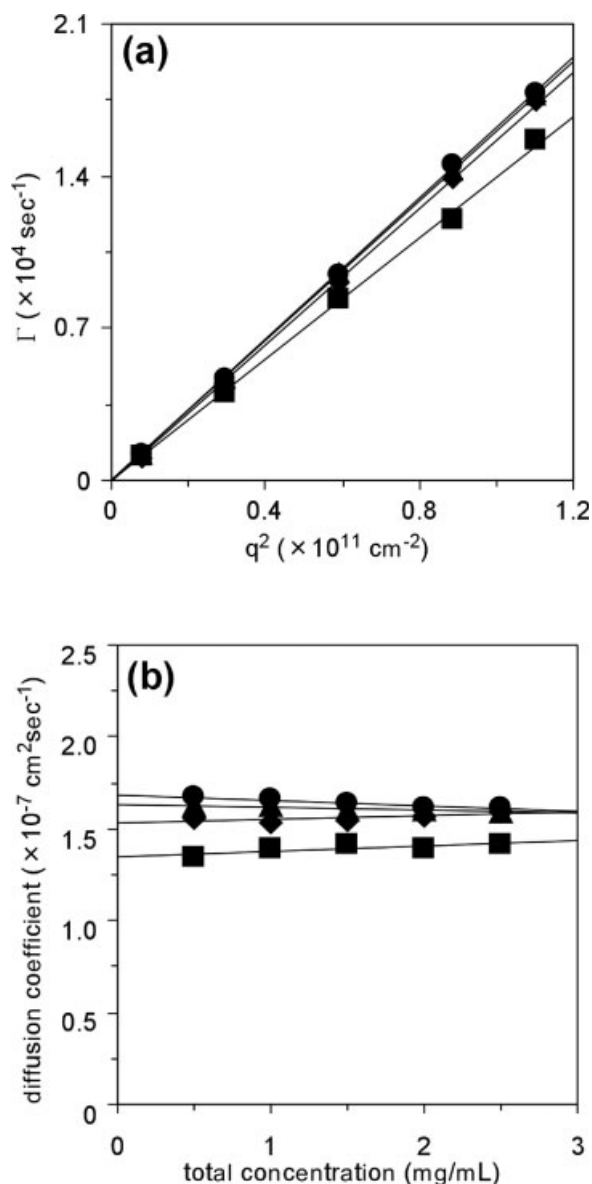


Figure 5. Estimation of PIC micelles using the cumulant DLS analysis: (a) angular dependence; (b) concentration dependence. (●, PEG₅-g-PAA; ▲, PEG₈-g-PAA; ■, PEG₁₂-g-PAA; ◆, PEG₁₇-g-PAA; detection angles, 30, 60, 90, 120, and 150° in (a) and 90° in (b); temperature, 25.0 ± 0.2 °C).

Assuming that the GOD/PEG-*g*-PAA complexes consist of a PIC core with a nonnegligible size and a PEG shell layer with a variance in the densities in the radial direction, it was reasonable to obtain R_g/R_h values of 0.720 to 0.745, which are close to a value for a hard sphere. Also, the mean diameter of GOD in light scattering measurement was $7 \pm 1 \text{ nm}$,¹³ and this size was influenced to micellar structure. When the association number of GOD increased, the R_g/R_h

R_h values also increased. This indicates the increase in the contribution of PIC core domain entrapping GOD molecules.

GOD catalyzes the oxidation of β -D-glucose to D-glucono-1, 4-lactone and hydrogen peroxide.¹⁰ The enzymatic activity of GOD incorporated in the core of the PIC micelles was examined using the peroxidase/*o*-dianisidine method.¹⁰ In this method, glucose as the substrate is oxidized to give D-glucono-1,4-lactone; and hydrogen peroxide is produced by the catalytic reaction of GOD. In the simultaneous second reaction, hydrogen peroxide is catalytically reduced by horseradish peroxidase in the presence of *o*-dianisidine, which then becomes oxidized to a red-brown dimer. The enzymatic activity of GOD is determined by measuring the amount of oxidized *o*-dianisidine that is produced. Figure 6 shows the relative activities of GOD-incorporated PIC micelles with PEG-*g*-PAA of various PEG contents against that of native GOD. Obviously, GOD in the PIC micelles exhibited comparable enzymatic activities with that of native GOD. It should be noted that there was a possibility that the micelle-incorporated GOD and small amount of un-incorporated GOD might be coexisted due to the critical association property of the micelles in the micelle solution. For GOD/PEG-*g*-PAA micelles, it is difficult to exhibit comparable enzymatic activity with native GOD from only un-incorporated GOD, and micelle-incorporated GOD might also show its activity even in the micelle. Glucose used as a substrate could easily diffuse into the core of the micelles. Glucose was catalyzed by GOD, and the reaction product diffused to the outer micelles. Indeed, in the case of lysozyme/PEG-P(Asp) micelles, the lysozyme in the micelles exhibits its enzymatic activity using a series of *p*-nitrophenyl-*N*-acetyl- β -chitooligosides (NAGs) with varying chain

Table 2. Diffusion Coefficients at the Infinite Dilution and Hydrodynamic Radius of GOD/PEG-*g*-PAA Complexes

Graft Copolymer	D_0 [$10^7 \text{ cm}^2/\text{s}$] ^a	R_h [nm] ^b
PEG ₅ -g-PAA	1.685	14.5
PEG ₈ -g-PAA	1.636	15.0
PEG ₁₂ -g-PAA	1.349	18.2
PEG ₁₇ -g-PAA	1.527	16.1

^a Determined from Figure 4(b).

^b Calculated from D_0 (second column) using the Stokes-Einstein equation (eq 6).

Table 3. Light Scattering Data for the GOD/PEG-*g*-PAA Complexes

Graft Copolymer	$M_{w,app}^a$ [g/mol]	Association Number ^b		R_g^a [nm]	R_g/R_h^c	A_2^a [mol L/g ²]
		GOD	PEG- <i>g</i> -PAA			
PEG ₅ - <i>g</i> -PAA	3,103,000	14	6	10.8	0.745	$8.302 \cdot 10^{-6}$
PEG ₈ - <i>g</i> -PAA	2,465,000	10	4	11.0	0.730	$1.428 \cdot 10^{-5}$
PEG ₁₂ - <i>g</i> -PAA	2,354,000	9	4	13.3	0.728	$1.485 \cdot 10^{-5}$
PEG ₁₇ - <i>g</i> -PAA	1,464,000	5	2	12.6	0.720	$2.522 \cdot 10^{-5}$

^a Determined from Zimm plots of SLS.

^b Calculated from $M_{w,app}$ (second column) and M_n of PEG-*g*-PAA (Table 1) and GOD (186,000 g/mol).

^c Calculated from R_g (fifth column) and R_h (Table 2).

lengths, that is, (NAG)₂, (NAG)₃, (NAG)₄, and (NAG)₅, as substrates.¹⁴ However, the enzymatic activity of the lysozyme in *Micrococcus luteus cells*, which are significantly larger (1–2 μm) in size compared with the micelles, was completely inhibited through the entrapment into the micelles.¹⁵ The glucose molecule is smaller than that of (NAG)₂, and glucose could easily penetrate into the core of the micelles. The diffusion of the substrate into the micelles might not become a rate-limiting process due to the small size of the micelles.

CONCLUSIONS

GOD-incorporated PIC micelles were prepared through the electrostatic interactions between

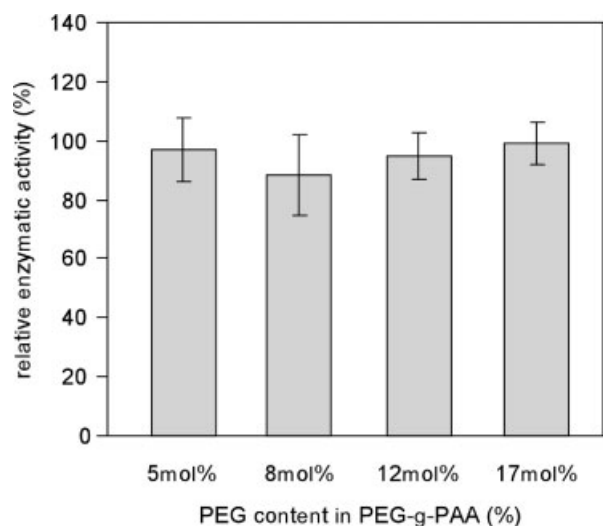


Figure 6. Relative enzymatic activity of GOD-incorporated PIC micelles with PEG-*g*-PAA having various PEG contents. The PIC micelles were prepared at stoichiometric MR (MR = 0.5). The data presented averages of three experiments ± SD.

glucose oxidase and PEG-*g*-PAA, which was synthesized through the reaction between PEG-NPC and PAA. GOD/PEG-*g*-PAA complexes prepared at a stoichiometric MR were small in size (ca. 30 nm) with a spherical particle, and formed a core-shell structure, in which the PIC core was formed from GOD, and the PAA main chain of PEG-*g*-PAA was surrounded by PEG graft chains. The size of the GOD/PEG-*g*-PAA complexes was determined by the thermodynamical balance between polyion complexation force and steric repulsive force. In addition, there was no decrease in the enzymatic activity of GOD in the core of the PIC micelles, and this was expected for the application of bionano-reactors and biosensors in biomedical fields. Furthermore, the GOD/PEG-*g*-PAA micelles studied here contained an acetal group, which can convert to a reactive group, that is, an aldehyde group, by mild acid treatment, at the tethered chain end of the PEG graft chain, and also has the potential ability to act as a starting element to construct a supramolecular architecture.

The authors thank Prof. Takashi Miyata, Kansai University, for kindly allowing us to use DLS-7000K for static light scattering measurements. This study was partly supported by the Sasakawa Scientific Research Grant from The Japan Science Society and a Grant-in-Aid for Scientific Research from the Ministry of Education, Science, Sports, and Culture in Japan.

REFERENCES AND NOTES

- (a) Yow, H. N.; Routh, A. F. *Soft Matter* 2006, 2, 940–949; (b) Ma, Y. J.; Dong, W. F.; Hempenius, M. A.; Mohwald, H.; Vancso, G. J. *Nat Mater* 2006, 5, 724–729; (c) Hammond, P. T. *Adv Mater* 2004, 16, 1271–1293; (d) Bertrand, P.; Jonas, A.; Laschewsky, A.; Legras, R. *Macromol Rapid Commun* 2000, 21, 319–348.

2. Harada, A.; Kataoka, K. *Prog Polym Sci* 2006, 31, 949–982.
3. (a) Harada, A.; Kataoka, K. *Macromolecules* 1995, 28, 5294–5299. (b) Harada, A.; Kataoka, K. *Science* 1999, 283, 65–67.
4. (a) Harada, A.; Kataoka, K. *Macromolecules* 2003, 36, 4995–5001; (b) Kabanov, A. V.; Bronich, T. K.; Kabanov, V. A.; Yu, K.; Eisenberg, A. *Macromolecules* 1996, 29, 6797–6802; (c) Bronich, T. K.; Popov, A. M.; Eisenberg, A.; Kabanov, V. A.; Kabanov, A. V. *Langmuir* 2000, 16, 481–489; (d) Kabanov, A. V.; Bronich, T. K.; Kabanov, V. A.; Yu, K.; Eisenberg, A. *J Am Chem Soc* 1998, 120, 9941–9942; (e) Gohy, J. F.; Varshney, S. K.; Antoun, S.; Jerome, R. *Macromolecules*, 2000, 33, 9298–9305; (f) Harada, A.; Kataoka, K. *Macromolecules* 1998, 31, 288–294.
5. Kataoka, K.; Harada, A.; Nagasaki, Y. *Adv Drug Deliv Rev* 2001, 47, 113–131.
6. Sotiropoulou, M.; Bokias, G.; Staikos, G. *Biomacromolecules*, 2005, 6, 1835–1838.
7. (a) Park, T. G.; Jeong, J. H.; Kim, S. W. *Adv Drug Deliv Rev* 2006, 58, 467–486; (b) Maruyama, A.; Ueda, M.; Kim, W. J.; Akaike, T. *Adv Drug Deliv Rev* 2001, 52, 227–233; (c) Bennis, J. M.; Kim, S. W. *J Drug Target* 2000, 8, 1–12; (d) Schuler, M.; Trentin, D.; Textor, M.; Tosatti, S. G. P. *Nanomedicine* 2006, 1, 449–463.
8. Harada, A.; Kataoka, K. *Langmuir* 1999, 15, 4208–4212.
9. Nagasaki, Y.; Kutsuna, T.; Iijima, M.; Kato, M.; Kataoka, K.; Kitano, S.; Kodama, Y. *Bioconjug Chem* 1995, 6, 231–233.
10. Frederick, K. R.; Tung, J.; Emerick, R. S.; Masiarz, F. R.; Chamberlain, S. H.; Vasavada, A.; Rosenberg, S.; Chakraborty, S.; Schopfer, L. M.; Massey, V. *J Biol Chem* 1990, 265, 3793–3802.
11. Berret, J.-F. *Macromolecules* 2007, 40, 4260–4266.
12. Douglas, J. K.; Roovers, J.; Freed, K. F. *Macromolecules* 1990, 23, 4168–4180.
13. Kamyshny, A.; Danino, D.; Magdassi, S.; Talmon, Y. *Langmuir*, 2002, 18, 3390–3391.
14. (a) Harada, A.; Kataoka, K. *J Controlled Release* 2001, 72, 85–91; (b) Harada, A.; Kataoka, K. *J Am Chem Soc* 2003, 125, 15306–15307.
15. Harada, A.; Kataoka, K. *J Am Chem Soc* 1999, 121, 9241–9242.